

Simulation of a Surface Transverse Wave Biosensor for DF-1 Cells

Nadira Jamil, Anis Nurashikin Nordin and
 Maizirwan Mel
 Faculty of Engineering,
 International Islamic University Malaysia,
 Kuala Lumpur, Malaysia
 dirajh@gmail.com

Ioana Voiculescu
 Department of Mechanical Engineering,
 The City College of New York,
 New York, USA

Abstract— A 250MHz Surface-Transverse Wave (STW) resonator is employed as a sensor element for the detection of DF-1 cells. STWs are horizontally polarized shear waves which are generated and detected by the interdigitated transducers (IDTs) similar to surface-acoustic wave (SAW) resonators. Detection of chemical and biological agents in aqueous solutions is a difficult problem, especially when the detection technique has to be sensitive, power-efficient and very handy. This paper presents the biosensor prototype utilizing STW resonator. The two-dimensional finite element (FEM) modeling of the STW resonator was performed using COMSOL Multiphysics™. 200MHz operating frequency was applied in the simulation. The FEM simulations results are equal with the theoretical results where an operating frequency of 200MHz will produce a resonance frequency of 200MHz.

Keywords- *Surface-transverse wave (STW), resonance frequency, interdigital transducers (IDTs), DF-1 cells, finite element method (FEM)*

I. INTRODUCTION

Acoustic wave sensors have recently received a lot attention due to their high sensitivity. These sensors utilize an acoustic wave propagating through or on the surface of a piezoelectric material, as its sensing mechanism. Any variations to the characteristics of the propagation path affect the velocity or amplitude of the wave.

Biosensor technology can enable investigators to detect amounts of biological samples. A biosensor comprises a biochemical recognition system and a transducer which will transform the biochemical response into an output signal to be measured [1-2]. In order to permit the usage of an acoustic wave based resonators as a biosensor, the device has to be coated with a biochemical layer corresponding to the analyte to be detected.

Being part of the surface acoustic waves (SAWs) family, surface transverse wave (STW) device focuses its energy on

the surface thus make it a more sensitive sensor [3]. Input and output transducers are being used to launch and receive the propagating acoustic surface wave [4] as illustrated in Figure 1. The input transducers transform the input electrical signal into mechanical acoustic waves and the reverse occurs at the output.

The STW properties include high propagation velocity, larger Q-values than surface acoustic wave (SAW) and bulk acoustic wave (BAW) devices, high power handling ability as well as low vibration sensitivity [5]. Fig. 1 illustrates the structure of an STW resonator. An STW device consists of a piezoelectric substrate with two interdigital transducers (IDTs); as input and output ports on top of the piezoelectric surface.

These IDTs are in the shape of two interlaced combs as exemplified in Fig. 2 where λ is the gap between the fingers. The propagation of surface transverse waves on piezoelectric substrates has been widely utilized in designing high frequency delay lines and resonators [6]. Resonance frequency can be obtained using $v = f\lambda$ where λ is equal to the spacing of the IDTs and v is the acoustic wave velocity [7].

II. EASE OF USE

To illustrate the application of the STW resonator as a biosensor, we have chosen to model the effect of loading DF-1 cells on the STW resonator. DF-1 is a continuous cell line of chicken embryo fibroblasts (CEF) [8] derived from 10-day old East Lansing Line (ELL-0) eggs. The cells have enhanced growth potential compared to secondary embryo fibroblast and are useful as substrates for virus propagation, recombinant protein expression and recombinant virus production.

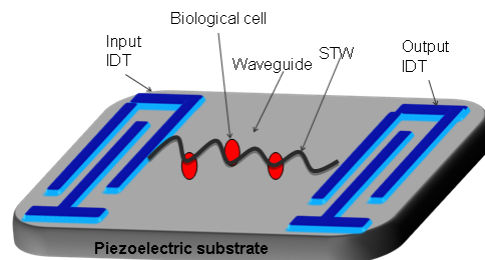


Figure 1. STW device structure

This work was supported in part by the NSF-EAGER award number 0940111, Brain Gain Malaysia Incentive: MOSTI/BGM/R&D/500-2/6(2) and the Fundamental Research Grant: FRGS 0308-90 provided by the Ministry of Higher Education of Malaysia.

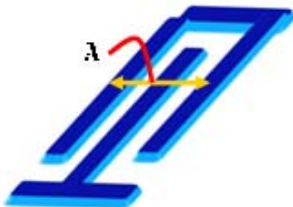


Figure 2. Interlaced combs of STW

Fig. 3 illustrates a microscopic image of the DF-1 cells. Current methods of cell detection and counting require scientific expertise, expensive and bulky equipment and take hours to complete. The usage of acoustic biosensors can drastically speed up this process. An added advantage is that this method requires inexpensive equipment and can be utilized by untrained personnel.

In this paper, a new design of an STW biosensor with a resonance frequency of 200 MHz is discussed followed by the simulation method. We used lithium niobate for the piezoelectric substrate while the IDTs are made of aluminium fingers. COMSOL MultiphysicsTM was used as the simulation software. Section II illustrates the Model Definition, Section III provides the simulation results for the designed biosensor and finally Section IV concludes the paper.

II. THEORY AND MODEL DEFINITION

The finite element method (FEM) has frequently been used to design acoustic wave structures such as transducers and resonators to obtain a desired frequency response [9]. Using this method, the STW resonator is divided into smaller elements and the integral formulation of each element is applied to form and approximated continuous function. The COMSOL MultiphysicsTM finite element solver was used to generate such functions and to predict the resonant frequency of the device.

The cross-section of STW device can be visualized as a two-dimensional rectangle with dimensions 1.2 μm X 0.2 μm as shown in Fig. 4. The lithium niobate piezoelectric layer, R1 acts as the substrate while the IDTs are formed using aluminium, CO1 for the input IDTs and CO2 for the output IDTs, respectively. The dimensions for both electrodes were 0.04 μm wide and 0.02 μm long.

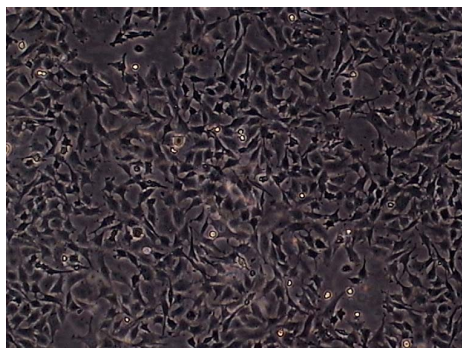


Figure 3. DF-1 cells

An electrical input of 5 V was placed at the input IDT to activate the inverse piezoelectric effect, where the applied potential difference induces mechanical deformations in the crystal. It is assumed that all the mechanical deformations will occur only at the piezoelectric substrate and the metal IDTs will act as a rigid body or defined as a decoupled, isotropic material.

The solver computes the mechanical deformations based on the piezoelectric stress charge constitutive relations, defined in COMSOL MultiphysicsTM as such:

$$\sigma = c_E \epsilon - e^T E \quad (1)$$

$$D = e\epsilon + \epsilon_0 \epsilon_{rs} E \quad (2)$$

In the above equations, σ and ϵ represent mechanical stress and strain, while D and E represent the electric displacement and field vectors respectively. The c_E is the elasticity matrix, whose values are shown in Table 1. Table 2 itemizes the values for the coupling e matrix (stress-charge form) for Lithium Niobate, while Table 3 shows relative permittivity matrix, ϵ_{rs} in the stress charge form.

The electrodes will be modeled as fine so that fewer elements are needed to accurately capture required aspects. Fewer elements also mean lower memory consumptions and a rapid computation time.

III. SIMULATION RESULTS

Acoustic wave propagation in the STW resonator can be modeled by equations from linearized fluid dynamics and solid dynamics [10]. The frequency response analysis in COMSOL MultiphysicsTM assumes that all equations are time dependent.

Harmonic excitations however, are defined as $\hat{f} = f e^{i\omega t}$, allowing the output response to be also harmonic and eliminating the time variable completely. Frequency domain simulations are preferred in COMSOL MultiphysicsTM since time domain simulations are obtained by applying an inverse Fourier transform.

For the STW resonator, frequency domain analysis was performed by applying 5 V to one set of the input IDTs as shown in Fig. 4. Applying such voltage in frequency domain indicates that a sinusoidal voltage with amplitude of 5 V is applied at the input IDTs. Due to the electric field, the piezoelectric layer underneath the IDTs will undergo deformations. The displacement results at each point of time can be defined as the real form of:

$$u = u_{amp} \cos(2\pi f t + u_{phase}) \quad (3)$$

where u_{amp} is the amplitude and u_{phase} is the phase of the displacement wave respectively. The simulation results indicating the displacement of the piezoelectric material is shown in Fig. 5.

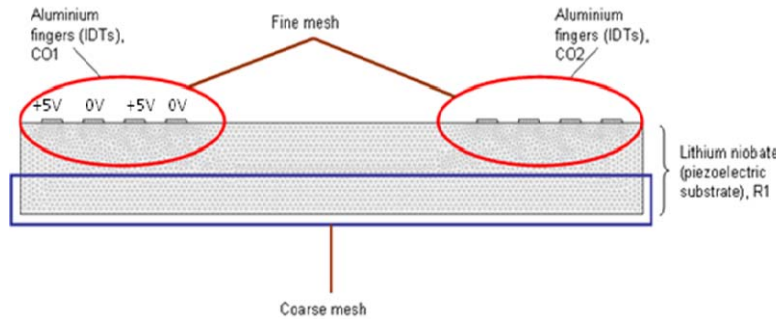


Figure 4. Mesh diagram

TABLE I. ELASTICITY MATRIX OF LITHIUM NIOBATE (LiNbO_3)

x	y	z	yz	xz	xy
2.02897e+11Pa	5.29177e+10Pa	7.49098e+10Pa	8.99874e+9Pa	0Pa	0Pa
	2.02897e+11Pa	7.49098e+10Pa	-8.99874e+9Pa	0Pa	0Pa
		2.43075e+11Pa	0Pa	0Pa	0Pa
			5.99034e+10Pa	0Pa	0Pa
				5.99018e+10Pa	8.98526e+9Pa
					7.43772e+10Pa

TABLE II. COUPLING MATRIX OF LITHIUM NIOBATE (LiNbO_3)

0C/m ²	0C/m ²	0C/m ²	0C/m ²	3.69594 C/m ²	-2.53384 C/m ²
-2.53764 C/m ²	2.53764 C/m ²	0C/m ²	3.69548 C/m ²	0C/m ²	0C/m ²
0.193644 C/m ²	0.193644 C/m ²	1.30863 C/m ²	0C/m ²	0C/m ²	0C/m ²

TABLE III. RELATIVE PERMITIVITY MATRIX OF LITHIUM NIOBATE (LiNbO_3)

43.6	0	0
	43.6	0
		29.16

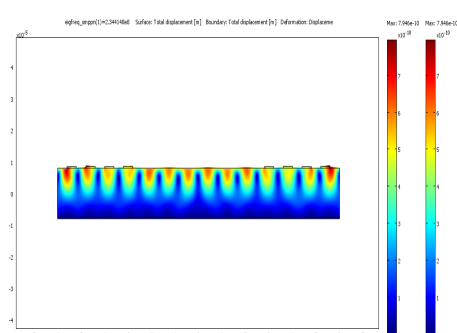


Figure 5. Cross-section of the 2-port STW resonator for frequency-domain analysis

Frequency domain analysis can also be used to obtain the eigenmodes and eigenfrequencies of the device which represent the resonant modes and frequencies of the device respectively. A resonance frequency at 200 MHz is expected for our STW structure considering $v = f\lambda$ where $\lambda = 16\mu\text{m}$ is equal to the spacing of the IDTs and $v = 3488\text{ms}^{-1}$ is the acoustic wave velocity for lithium niobate. To observe this, the eigenfrequency analysis was performed for the frequency ranging between 150MHz to 250MHz. The simulation results illustrating the resonance frequency of the STW resonator is shown in Figure 6.

The frequency response shown in Figure 6 also allows us to calculate the Q-factor of the device. Q-factor is a measure of the ratio between stored energy and energy lost per cycle. COMSOL Multiphysics™, evaluates the Q-factor the following equation:

$$Q = \frac{\omega \times m \times h_0}{\eta \times A} \quad (4)$$

where h_0 =film thickness, η =dynamic viscosity, A =slide film area, m =proof mass and ω =resonance frequency[11]. From the simulation, Q-factor is found to be 2999.

TABLE IV. PROPERTIES OF WATER

Young's Modulus	2.0e11Pa
Poisson's ratio	0.33
Density	$\rho(T[1/K])[kg/m^3]$

The Q factor can also be obtained from the graph shown in Fig. 6, where resonance frequency, f_0 is 200MHz and the bandwidth, $f_2 - f_1 = 0.001MHz$. Using this method, the Q factor is 2000 as shown in the calculation below.

$$\frac{f_0}{(f_2 - f_1)} = \frac{200MHz}{(2.0005MHz - 1.9995MHz)} = 2000$$

In order to achieve the objective, the structural settings of lithium niobate had to be defined. These settings are its elasticity matrix, coupling matrix and relative permittivity. It is crucial to identify these items as without them, it is impossible to have the simulation working successfully.

There are a few properties related to DF-1 cells that have to be taken into account such as its Young's modulus, Poisson's ratio and density. Since these properties are yet to be discovered, we had water as a substitution to DF-1 cells in the simulation. Table 4 summarizes the properties of water used in the simulation.

Figure 7 illustrates the result of the simulation. From the simulation, Q-factor is found to be 1999. Figure 8 defines the Q factor based on the graph and the Q-factor calculated is 1836.

IV. CONCLUSION

A two-port STW resonator was simulated using COMSOL Multiphysics™. The device had the following dimensions 1.2 μm X 0.2 μm . The FEM simulations allowed us to obtain the resonant frequency of 200MHz and Q factor of 2000. The obtained results from the design model agree with the

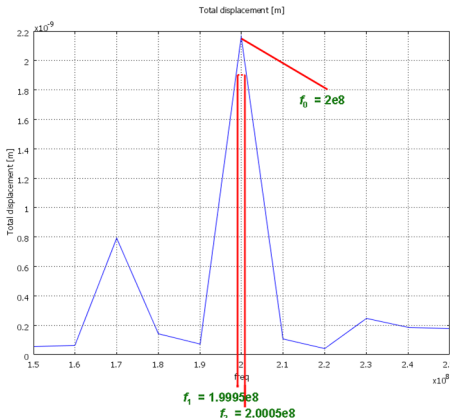


Figure 6. Graph of the resonance frequency to calculate the Q-factor

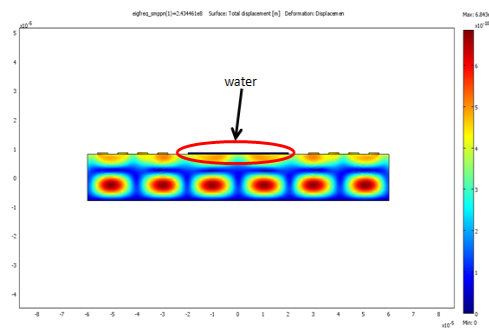


Figure 7. Cross-section of the 2-port STW resonator (with water droplets) for frequency-domain analysis

calculated measurements thus it is proved that COMSOL Multiphysics™ can be used to simulate STW devices.

ACKNOWLEDGMENT

This work is a collaboration between International Islamic University Malaysia and City College of New York and is funded by the MOSTI's Brain Gain Programme: MOSTI/BGM/R&D/500-2/6(2), MOHE's Fundamental Research Grant: FRGS 0308-90 and also by the Professional Staff Congress of City University of New York (PSC-CUNY), Research Award Program PSCREG-39-685.

REFERENCES

- [1] Cavic, B.A., Hayward, G.L., Thompson, M., . "Acoustic waves and the study of biochemical macromolecules and cells at the sensor-liquid interface, Analyst no. 124, 1999, 1405-1420.
- [2] Janshoff, A., Galla, H.-J., Steinem, C., "Piezoelectric mass sensing devices as biosensors- an alternative to optical biosensors" (2000). Angewandte Chemie International Edition 39, 4004- 4032.
- [3] Bill Drafts, "Acoustic wave technology sensors", presented at Microwave Theory and Techniques, 2001. Proceedings of IEEE, 2001
- [4] <http://www.visensors.com>
- [5] Avramov Ivan D., High-performance surface transverse wave resonators in the lower GHz frequency range. Institute of Solid State Physics, Bulgaria (2000)
- [6] Daniel F. Thompson and B. A. Auld, "Surface transverse wave propagation under metal strip gratings", IEEE Ultrasonics symposium. (1986)
- [7] G. Scheerschmidt, K.J. Kirk1 and G. McRobbie, "Finite element

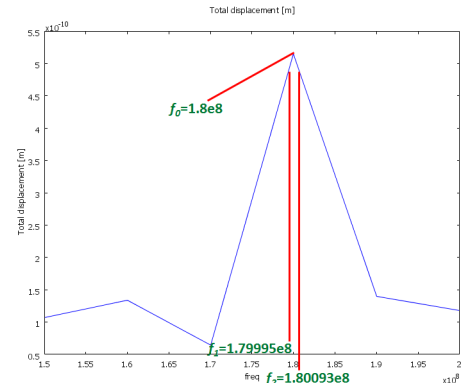


Figure 8. Graph of the resonance frequency to calculate the Q-factor for simulation in Fig. 7

- analysis of resonant frequencies in surface acoustic wave devices”,
Proceedings of the COMSOL Users Conference. (2006)
- [8] Himly M, Foster DN, Bottoli I, Iacovoni JS, Vogt PK. “The DF-1 chicken fibroblast cell line: transformation induced by diverse oncogenes and cell death resulting from infection by avian leukosis viruses”. Department of Molecular and Experimental Medicine, The Scripps Research Institute, 10550 North Torrey Pines Road, La Jolla, California, 92037, USA.
 - [9] Nordin, A. N. & Zaghloul, M. E. (2007) Modeling and fabrication of CMOS surface acoustic wave resonators. IEEE Transactions on Microwave Theory and Techniques, 55, 992-1001.
 - [10] MEMS Module, COMSOL Multiphysics™, 2008
 - [11] Estimating the Q factor of a MEMS Gyroscope, COMSOL Multiphysics™, 2008